CHEMIJA. 2015. Vol. 26. No. 3. P. 165–169

Graphene and niobium(V) oxide/graphene supported platinum–cobalt catalysts as cathode material for oxygen reduction

Virginija Kepenienė*,

Raminta Stagniūnaitė,

Loreta Tamašauskaitė-Tamašiūnaitė,

Irena Stalnionienė,

Eugenijus Norkus

Center for Physical Sciences and Technology,
A. Goštauto St. 9,
LT-01108 Vilnius, Lithuania

The paper describes fabrication of the graphene and Nb_2O_5/graphene supported Pt or PtCo nanoparticles catalysts by means of microwave synthesis. The electrocatalytic activities of the synthesized catalysts towards the reduction of oxygen were investigated by linear scan voltammetry.

It has been found that the graphene and Nb_2O_5/graphene supported PtCo nanoparticles catalysts show exhibited electrocatalytic efficiency towards the reduction of oxygen when compared with that of bare Pt/GR catalyst.

Key words: platinum–cobalt, niobium(V) oxide, electrocatalysts, oxygen reduction

INTRODUCTION

The electrocatalytic oxygen reduction reaction (ORR) is an important process in energy converting systems such as low temperature proton exchange membrane fuel cells (PEMFCs) [1]. Therefore, understanding oxygen reduction mechanistic pathways in terms of developing an efficient and stable catalyst has been the main research interest over several decades.

One of the most important problems related to the ORR is the complex and strong kinetic inhibition that leads to high over-potentials under PEMFCs operating conditions. It is thus utterly important to develop more efficient catalysts and understand key factors controlling their activity. Platinum-supported carbon or high-surface-area carbon (e. g. black carbon, Vulcan X-72) are one of the most widely used catalysts as a cathode in low temperature fuel cells. However, the degradation and corrosion of carbon support under the cathode working conditions in PEMFCs are a major cause to lose the cell performance during their operation [2–4]. It was described that adding of transition metals to the Pt-based catalysts, like Co [5–24], Ni [5, 6, 23–25], Fe [5, 8, 21, 24, 26], Cr [12], Cu [27–31], enhances electrocatalytic properties of catalysts as compared to those of bare Pt catalysts and allows reducing the Pt amount in the catalyst. The catalytic enhancement of Pt with transition metals has been attributed to the PtM alloy formation and the Pt electronic structure change due to the presence of metal, Pt-Pt interatomic distance [32], reducing the Pt-O formation during the inhibition of molecular oxygen reduction [8], exposure of more active vicinal plane on dispersed platinum particles [33] and increasing the 5d-electron vacancy which results in increased molecular oxygen adsorption and weakening of the O-O bond [5].

Similarly, composite Pt-based electrocatalysts containing rare earth or transition metal oxides, such as Nb_2O_5 [34, 35], CeO_2 [36–39] and TiO_2 [40–42], have exhibited a number of characteristics that make them interesting for catalytic studies due to the synergetic electronic effect. The use of graphene (GR) as a catalyst support can also improve the activity and stability of catalysts towards the reduction of oxygen [43–46].

In this study we investigated the graphene and Nb_2O_5/graphene supported PtCo nanoparticles catalysts (denoted as PtCo/GR and PtCoNb_2O_5/GR) for their ORR performance, whereas in our previous study those catalysts were identified as good catalysts for the electro-oxidation of ethanol [47, 48]. The catalysts were prepared by a fast and simple rapid microwave irradiation method, which allows producing catalysts with a small particle size and high distribution on the support and with tailored properties.

* Corresponding author. E-mail: virginalisk@gmail.com

EXPERIMENTAL

Chemicals

H_2PtCl_6 (99.9%), $CoCl_2 \cdot 6H_2O$ (98%) and Nb_2O_5 powder (99.9%) were purchased from Alfa-Aesar and Sigma-Aldrich Supplies. Graphene (GR) (purity of 97%, specific surface area 60 m^2g^{-1}) was purchased from Graphene Supermarket Supply. Nafion (5 wt.%, D521, 1100 EW) was purchased from Ion Power Inc. H_2SO_4 (96%), NaOH (98.8%), ethylene glycol (EG) and acetone were purchased from Chempur Company. Oxygen (99.999%) was used for the saturation of H_2SO_4 solution. All chemicals were of analytical grade. Ultra-pure water with the resistivity of 18.2 MΩ cm^{-1} was used to prepare all the solutions.

Preparation of catalysts

The catalysts were prepared by means of microwave synthesis. PtCo/GR catalyst was prepared by microwave-assisted heating of ethylene glycol (EG) solutions of Pt(IV) and Co(II) salts as was described in Ref. [47]. A typical preparation consists of the following steps: 0.25 ml of 0.096 M H_2PtCl_6 and 0.6 ml of the calculated concentration of $CoCl_2$ solution were mixed with 18 ml of EG. Then, pH of the solution was adjusted to 11.7 by adding dropwise a 1 M NaOH solution. 100 mg of graphene was added to the mixture and sonicated for 30 min. For the microwave irradiation, the reaction mixture was put into a Monowave 300 microwave reactor (Anton Paar). The reduction of PtCo nanoparticles was carried out at a temperature of 170 °C for 30 min.

The $PtCoNb_2O_5$/GR catalyst was prepared in the same manner, only the base support was 100 mg dry niobium oxide powder mixed with graphene powder, with the mass ratio being 1 : 1 [48].

For comparison, the graphene supported Pt catalyst was also prepared in the same manner by heating of EG solution of Pt(IV) salt at 170 °C for 30 s. The duration of Pt/GR preparation was shortened to 30 s with the aim to compare the obtained PtCo/GR, $PtCoNb_2O_5$/GR and Pt/GR catalysts having approximately the similar size of Pt particles in the created catalysts. After preparation, the synthesized catalysts were washed with acetone, ultra-pure water, then filtered and dried in a vacuum oven at 80 °C for 2 h.

Characterization of catalysts

The Pt and Co metal loadings were estimated by means of Inductively Coupled Plasma Optical Emission Spectroscopy (ICP-OES). The ICP optical emission spectra were recorded using an ICP optical emission spectrometer Optima 7000DV (Perkin Elmer).

Electrochemical measurements

A conventional three-electrode cell was used for electrochemical measurements. The working electrode was a thin layer of a Nafion-impregnated catalyst cast on a glassy carbon electrode with a geometric area of 0.07 cm^2. A Pt sheet was used as a counter electrode and an Ag/AgCl/KCl electrode was used as a reference. The catalyst layer was obtained according to the following steps: at first, the required amounts of the PtCo/GR, $PtCoNb_2O_5$/GR or Pt/GR catalysts were dispersed ultrasonically for 1 hour in a solution containing 0.25 μl of 5 wt.% Nafion and 0.75 μl deionized H_2O to produce a homogeneous slurry. Then 5 μl of the prepared suspension mixture was pipetted onto the polished surface of a glassy carbon electrode and dried in air for 12 h.

All electrochemical measurements were performed with Zennium (ZAHNER-Elektrik GmbH & Co. KG) and AUTOLAB electrochemical workstations. For the ORR measurements the working electrode was pretreated electrochemically over a potential range of 0–1.5 V with a scan rate of 50 mV s^{-1} for 30 min before each measurement. The electrochemically active surface areas (ESAs) of the prepared catalysts were determined from the integrated charge of the hydrogen adsorption region (Q_H) in the cyclic voltammograms and calculated according to Eq. (1) [49]:

$$\text{ESA } (cm^2) = Q_H\ (\mu C) / 220\ (\mu C\ cm^{-2}), \quad (1)$$

where 220 μC cm^{-2} is the charge required to oxidize a monolayer hydrogen adsorbed on Pt. ESA values ($m^2\ g^{-1}$) were calculated according to Eq. (2):

$$\text{ESA } (m^2\ g^{-1}) = Q_H/\text{Pt loading} \times 220. \quad (2)$$

Prior to the ORR experiments, the 0.5 M H_2SO_4 solution was purged with O_2 for 15 min. The ORR measurements were performed by linear scan voltammetry from 1.0 V to 0.7 V in the cathodic direction at 5 mV s^{-1} in the oxygen-saturated 0.5 M H_2SO_4 solution at a temperature of 25 °C. The electrode potential is quoted versus the standard hydrogen electrode (SHE). The presented current densities are normalized with respect to the geometric area of catalysts.

RESULTS AND DISCUSSION

The graphene and Nb_2O_5/graphene supported PtCo catalysts were prepared with Pt nanoparticles in a size of 2.0 and 1.3 nm, respectively [23, 24]. For comparison, the Pt/GR catalyst with the Pt nanoparticles in a size of ca. 5 nm was synthesized. In the case of the PtCo/GR catalyst, the formation of platinum solid solution in cobalt was detected by XRD [23]. It has been determined that the orthorhombic and monoclinic niobium(V) oxides were predominant in the $PtCoNb_2O_5$/GR catalyst [24].

The Pt loadings, determined by ICP-OES, were 0.143 mg Pt cm^{-2} in the Pt/GR and 0.165 and 0.285 mg Pt cm^{-2} in the synthesized PtCo/GR and $PtCoNb_2O_5$/GR catalysts, respectively. The electrochemically active surface areas of Pt in the synthesized catalysts were determined from the cyclic voltammograms of the Pt/GR, $PtCoNb_2O_5$/GR and PtCo/GR catalysts recorded in a deaerated 0.5 M H_2SO_4 solution at

a sweep rate of 50 mV s^{-1} by calculating the charge associated with hydrogen adsorption (220 μC cm^{-2}) (Fig. 1) [49]. It has been determined that the values of ESA are 4.8 cm^2 for Pt/GR and 4.8 and 4.3 cm^2 for the PtCo/GR and $PtCoNb_2O_5$/GR catalysts, respectively. The specific activity has been determined to be 48 $m^2\ g^{-1}$ Pt for Pt/GR, 42 $m^2\ g^{-1}$ Pt for PtCo/GR and 21 $m^2\ g^{-1}$ Pt for $PtCoNb_2O_5$/GR.

The reduction of oxygen was investigated at the PtCo/GR, $PtCoNb_2O_5$/GR and Pt/GR catalysts electrochemically pretreated in 0.5 M H_2SO_4 at 50 mV s^{-1} for 30 min. Figure 2 shows the ORR polarization curves of the investigated catalysts. The potential was scanned from ca. 1.0 V in the cathodic direction to 0.7 V vs SHE at a scan rate of 5 mV s^{-1}. According to the literature, at the potential between 0.7 and 0.9 V vs SHE the ORR response is dominated by the kinetics of electrocatalysts [50]. As seen from the data obtained, the Pt/GR catalyst performed lower ORR activity with the onset potential of 0.93 V, while the PtCo/GR and $PtCoNb_2O_5$/GR catalysts show higher onset potentials of 0.98 and 1.0 V, respectively, as well as higher ORR current densities (Fig. 2). The $PtCoNb_2O_5$/GR catalyst shows a more positive onset potential than the PtCo/GR and Pt/GR catalysts and a higher current in the mixed-kinetic-diffusion region (Fig. 2, dash-dotted line).

For the sake of comparison, the oxygen reduction current densities at the potential values of 0.85 and 0.75 V, respectively, were normalized by the Pt loadings and electrochemically active surface areas for each catalyst to represent mass activity (MA) and specific activity (SA), respectively. The summarized data are given in Table. Figure 3 presents a comparison of the mass (a) and specific (b) activities of Pt/GR, PtCo/GR and $PtCoNb_2O_5$/GR at 0.85 and 0.75 V, respectively. As evident, at a potential value of 0.85 V vs SHE the Pt-mass activity is ca. 1.5 and 1.9 times higher at PtCo/GR and $PtCoNb_2O_5$/GR, respectively, than that at Pt/GR. At 0.75 V, the Pt-mass activity is ca. 2.5 and 2.0 times greater at PtCo/GR and $PtCoNb_2O_5$/GR as compared with that at Pt/GR (Fig. 3a). Oxygen reduction current densities normalized by the electrochemically active surface areas recorded at 0.85 and 0.75 V are ca. 2.0 and 4.7 and 2.9 and 4.4 times higher at the PtCo/GR and $PtCoNb_2O_5$/GR catalysts, respectively, than those at Pt/GR (Fig. 3b).

When comparing the activity of the PtCo/GR and $PtCoNb_2O_5$/GR catalysts towards ORR, it is clearly seen that the higher current densities are obtained at $PtCoNb_2O_5$/GR. The introducing of Nb_2O_5 into the composition of PtCo catalyst increases its activity towards ORR. Oxygen reduction current

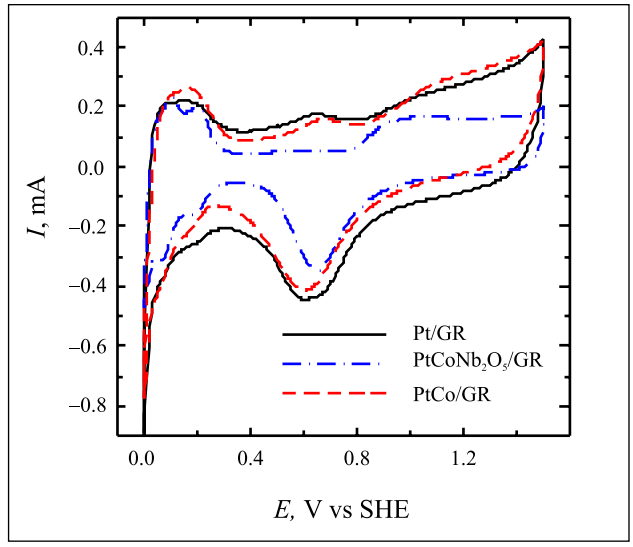

Fig. 1. Cyclic voltammograms of Pt/GR (*solid line*), $PtCoNb_2O_5$/GR (*dash-dotted line*) and PtCo/GR (*dashed line*) recorded in 0.5 M H_2SO_4 at 50 mV s^{-1}

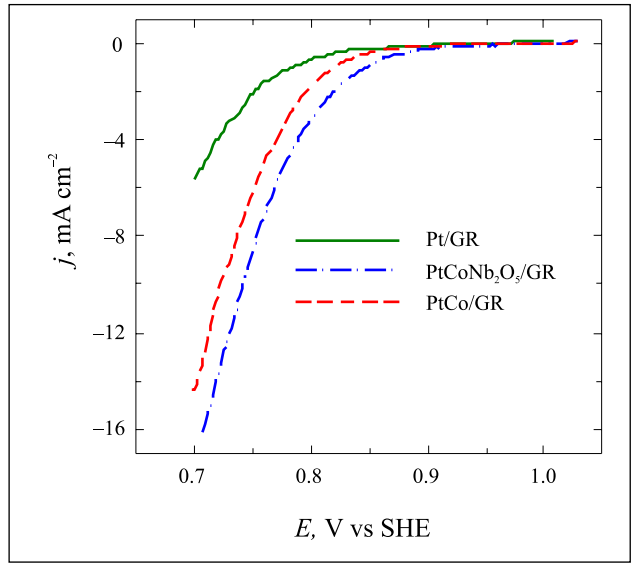

Fig. 2. Linear sweep voltammetry scans for Pt/GR (*solid line*), $PtCoNb_2O_5$/GR (*dash-dotted line*) and PtCo/GR (*dashed line*) recorded in the O_2-saturated 0.5 M H_2SO_4 solution at 5 mV s^{-1}

Table. **Summary of the results obtained from electrochemical measurements**

Catalysts	Onset potential, V	ESA, cm^2	Pt loading, mg cm^{-2}	Oxygen reduction			
				E, V	*j*, mA cm^{-2}	MA, mA mg_{Pt}^{-1}	SA, mA cm^{-2}
Pt/GR	0.93	4.8	0.143	0.85	0.23	1.61	0.003
				0.75	2.15	15.03	0.031
PtCo/GR	0.98	4.8	0.165	0.85	0.39	2.36	0.006
				0.75	6.12	37.09	0.089
PtCo-Nb_2O_5/GR	1.00	4.3	0.285	0.85	0.86	3.02	0.014
				0.75	8.50	29.82	0.138

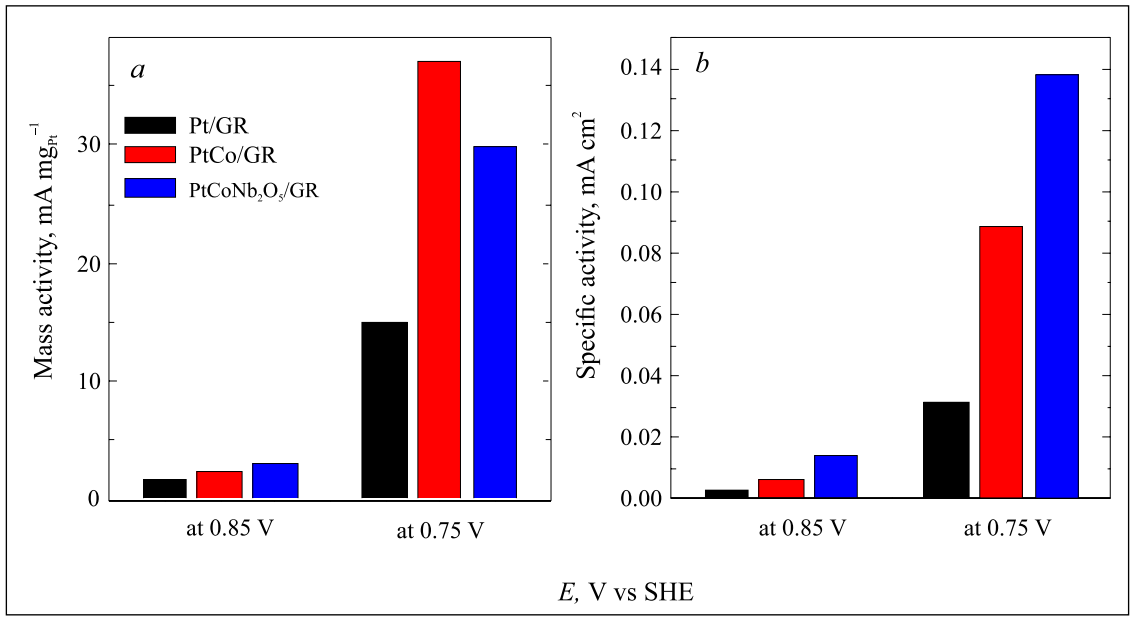

Fig. 3. Comparison of mass (*a*) and specific (*b*) activities for Pt/GR, PtCo/GR and $PtCoNb_2O_5$/GR at 0.85 and 0.75 V, respectively

densities at 0.75 V are ca. 1.4 times higher at $PtCoNb_2O_5$/GR than those at PtCo/GR (Fig. 2). The specific current density values at 0.75 V are also 1.6 times higher at the $PtCoNb_2O_5$/GR catalyst, whereas the mass activity is ca. 1.2 times greater at PtCo/GR than that at the $PtCoNb_2O_5$/GR catalyst (Fig. 3).

CONCLUSIONS

The graphene and Nb_2O_5/graphene supported PtCo catalysts prepared by means of microwave synthesis show enhanced activity towards the reduction of oxygen as compared with that at the bare Pt/graphene catalyst. The graphene and Nb_2O_5/graphene supported PtCo catalysts show higher onset potentials, as well as higher current densities towards oxygen reduction reaction as compared with those at the bare Pt/graphene catalyst.

ACKNOWLEDGEMENTS

V. Kepenienė acknowledges Postdoctoral Fellowship is being funded by the European Union Structural Funds Project "Postdoctoral Fellowship Implementation in Lithuania". R. Stagniūnaitė acknowledges support by the project "Promotion of Student Scientific Activities" (VP1-3.1-ŠMM-01-V-02-003) from the Research Council of Lithuania. This project is funded by the Republic of Lithuania and the European Social Fund under the 2007–2013 Human Resources Development Operational Programme's Priority 3.

Received 1 June 2015
Accepted 26 June 2015

References

1. Y. Nie, L. Li, Z. Wei, *Chem. Soc. Rev.*, **44**, 2168 (2015).
2. X. Yu, S. Ye, *J. Power Sources*, **172**, 145 (2007).
3. S. L. Candelaria, Y. Shao, W. Zhou, et al., *Nano Energy*, **1**, 195 (2012).
4. G. Zibao, Z. Xiuwen, W. Dailing, et al., *Superlattices Micros.*, **47**, 705 (2010).
5. T. Toda, H. Igarashi, H. Uchida, M. Watanabe, *J. Electrochem. Soc.*, **146**, 3750 (1999).
6. N. M. Markovic, T. J. Schmidt, V. Stamenkovic, P. N. Ross, *Fuel Cells*, **1**, 105 (2001).
7. J. R. C. Salgado, E. Antolini, E. R. Gonzalez., *J. Electrochem. Soc.*, **151(12)**, A2143 (2004).
8. V. S. Murthi, R. C. Urian, S. Mukerjee, *J. Phys. Chem. B*, **108**, 11011 (2004).
9. Q. Huang, H. Yang, Y. Tang, T. Lu, G. L. Akins, *Electrochem. Comm.*, **8**, 1220 (2006).
10. F. H. B. Lima, W. H. Lizcano-Valbuena, E. Teixeira-Neto, F. C. Nart, E. R. Gonzalez, E. A. Ticianelli, *Electrochim. Acta*, **52**, 385 (2006).
11. Q. Xu, E. Kreidler, T. He, *Electrochim. Acta*, **55**, 7551 (2010).
12. M. K. Jeon, Y. Zhang, P. J. McGinn, *Electrochim. Acta*, **55**, 5318 (2010).
13. Q. He, S. Mukerjee, *Electrochim. Acta*, **55**, 1709 (2010).
14. E. B. Fox, H. R. Colon-Mercado, *Int. J. Hydrogen Energy*, **35**, 3280 (2010).
15. S.-H. Liu, F.-S. Zheng, J.-R. Wu, *Appl. Catal., B*, **108–109**, 81 (2011).
16. R. Jiang, C. Rong, D. Chu, *Electrochim. Acta*, **56**, 2532 (2011).
17. M. V. Lebedeva, V. Pierron-Bohnes, C. Goyhenex, et al., *Electrochim. Acta*, **108**, 605 (2013).
18. G. Sievers, S. Mueller, A. Quade, et al., *J. Power Sources*, **268**, 255 (2014).
19. M. Yaldagard, N. Seghatoleslami, M. Jahanshahi, *Appl. Surf. Sci.*, **315**, 222 (2014).
20. J.-N. Zheng, L.-L. He, C. Chen, A.-J. Wang, K.-F. Ma, J.-J. Feng, *J. Power Sources*, **268**, 744 (2014).

21. C. Dominguez, F. J. Perez-Alonso, M. Abdel Salam, *Int. J. Hydrogen Energy*, **39**, 5309 (2014).
22. B. Li, Z. Yan, Q. Xiao, et al., *J. Power Sources*, **270**, 201 (2014).
23. C. A. Cortes-Escobedo, R. G. Gonzalez-Huerta, A. M. Bolarin-Miro, et al., *Int. J. Hydrogen Energy*, **39**, 16722 (2014).
24. W. Li, P. Haldar., *Electrochem. Solid-State Lett.*, **13(5)**, B47 (2010).
25. A. R. Malheiro, J. Perez, H. M. Villullas, *J. Electrochem. Soc.*, **156(1)**, B51 (2009).
26. M. Neergat, R. Rahul, *J. Electrochem. Soc.*, **159(7)**, F234 (2012).
27. H. El-Deeb, M. Bron, *Electrochim. Acta*, **164**, 315 (2015).
28. H. El-Deeb, M. Bron, *J. Power Sources*, **275**, 893 (2015).
29. J. Sun, J. Shi, J. Xu, X. Chen, Z. Zhang, Z. Peng, *J. Power Sources*, **279**, 334 (2015).
30. J. Liu, C. Xu, C. Liu, *Electrochim. Acta*, **152**, 425 (2015).
31. V. Jalan, E. J. Taylor, *J. Electrochem Soc*., **130**, 2299 (1983).
32. B. C. Beard, P. N. Ross, *J. Electrochem. Soc*., **137**, 3368 (1990).
33. A. Bonakdarpour, R. T. Tucker, M. D. Fleischauer, N. A. Beckers, M. J. Brett, D. P. Wilkinson, *Electrochim. Acta*, **85**, 492 (2012).
34. F. D. Kong, G.-P. Yin, C.-Y. Du, *Cat. Comm.*, **68**, 67 (2015).
35. K. H. Lee, K. Kwon, V. Roev, D. Y. Yoo, H. Chang, D. Seung, *J. Power Sources*, **185**, 871 (2008).
36. C.-W. Liu, Y.-C. Wei, K.-W. Wang, *Electrochem. Commun.*, **11**, 1362 (2009).
37. S. Chang, M. Li, Q. Hua, et al., *J. Cat.*, **293**, 195 (2012).
38. A. Altamirano-Gutierrez, A. M. Fernandez, F. J. Rodrıguez Varela, *Int. J. Hydrogen Energy*, **38**, 12657 (2013).
39. S. H. Kang, Y.-E. Sung, W. H. Smyrl, *J. Electrochem. Soc*., **155(11)**, B1128 (2008).
40. S. H. Kang, T.-Y. Jeon, H.-S. Kim, Y.-E. Sung, W. H. Smyrl, *J. Electrochem. Soc.*, **155(10)**, B1058 (2008).
41. K. Jukk, N. Kongi, A. Tarre, et al., *J. Electroanal. Chem.*, **735**, 68 (2014).
42. H.-J. Choi, S.-M. Jung, J.-M. Seo, D. W. Chang, L. Dai, J.-B. Baek, *Nano Energy*, **1**, 534 (2012).
43. A. A. Ensafi, M. Jafari-Asl, B. Rezaei, *Electrochim. Acta*, **130**, 397 (2014).
44. J.-N. Zheng, S.-S. Li, X. Ma, et al., *J. Power Sources*, **262**, 270 (2014).
45. A. Navaee, A. Salimi, S. Soltanian, P. Servati, *J. Power Sources*, **277**, 268 (2015).
46. V. Kepeniene, L. Tamašauskaite-Tamašiūnaite, J. Jablonskiene, J. Vaičiūniene, R. Kondrotas, R. Juškenas, E. Norkus, *J. Electrochem. Soc*., **161**, F1354 (2014).
47. V. Kepenienė, J. Vaičiūnienė, R. Kondrotas, V. Pakštas, L. Tamašauskaitė-Tamašiūnaitė, E. Norkus, *ECS Transactions*, **64**, 1147 (2014).
48. H. Angerstein-Kozlowska, B. E. Conway, W. B. A. Sharp, *J. Electroanal. Chem.*, **43**, 9 (1973).
49. U. Paulus, T. Schmidt, H. Gasteiger, R. Behm, *J. Electroanal. Chem.*, **495**, 134 (2001).

Virginija Kepenienė, Raminta Stagniūnaitė, Loreta Tamašauskaitė-Tamašiūnaitė, Irena Stalnionienė, Eugenijus Norkus

GRAFENO IR NIOBIO(V) OKSIDO / GRAFENO PAGRINDU SUSINTETINTŲ PLATINOS-KOBALTO KATALIZATORIŲ PANAUDOJIMAS KATODAIS DEGUONIES REDUKCIJOS REAKCIJAI

S a n t r a u k a

Mikrobangų sintezės metodu buvo suformuoti PtCo/grafeno, $PtCoNb_2O_5$/grafeno ir Pt/grafeno katalizatoriai. Nustatyta, kad nusodintos Pt įkrova susintetintuose PtCo/grafeno, $PtCoNb_2O_5$/grafeno ir Pt/grafeno katalizatoriuose yra lygi atitinkamai 0,165, 0,285 ir 0,143 mg cm^{-2}, o nusodintų Pt nanodalelių dydis minėtuose katalizatoriuose yra nuo 1 iki 5 nm.

Katalizatorių elektrochemiškai aktyvus paviršiaus plotas buvo nustatytas iš vandenilio monosluoksnio adsorbcijos ant Pt elektrodo krūvio 0,5 M H_2SO_4 tirpale, skleidžiant elektrodo potencialą 50 mV s^{-1} greičiu potencialų intervale nuo 0 iki 1,5 V (SHE). Nustatyta, kad PtCo/grafeno, $PtCoNb_2O_5$/grafeno ir Pt/grafeno katalizatorių elektrochemiškai aktyvus paviršiaus plotas yra lygus atitinkamai 4,8, 4,3 ir 4,8 cm^2.

Deguonies redukcija buvo tiriama O_2 prisotintame 0,5 M H_2SO_4 tirpale. Naudojant PtCo/grafeno ir $PtCoNb_2O_5$/grafeno katalizatorius, deguonies redukcija prasideda esant 0,98–1,0 V potencialui, o naudojant Pt/grafeno katalizatorių – esant 0,93 V potencialui. Deguonies redukcijos srovės tankio vertės, apskaičiuotos pagal nusodintos Pt įkrovą ir aktyvų paviršiaus plotą esant 0,75 ir 0,85 V potencialo vertėms, yra ženkliai didesnės ant PtCo/grafeno ir $PtCoNb_2O_5$/grafeno katalizatorių, palyginti su Pt/grafeno katalizatoriumi.